Chemical Science

Accepted Manuscript

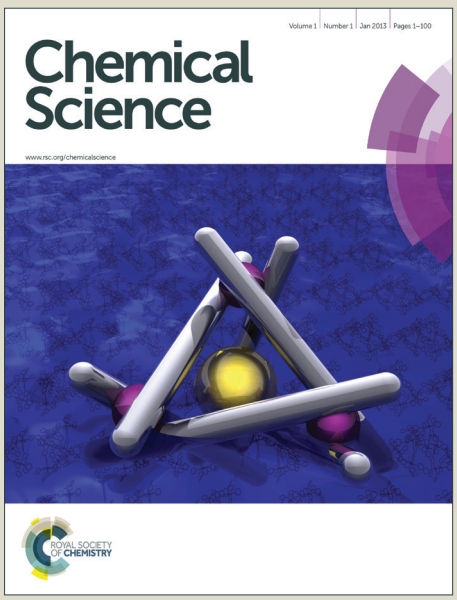

ROYAL SOCIETY OF CHEMISTRY

www.rsc.org/chemicalscience

Cite this: DOI: 10.1039/c0xx00000x

www.rsc.org/xxxxxx

PAPER

Thermally-labile segmented hyperbranched copolymers: Using reversible-covalent chemistry to investigate the mechanism of self-condensing vinyl copolymerization

Hao Sun, Christopher P. Kabb and Brent S. Sumerlin*

Received (in XXX, XXX) Xth XXXXXXXXX 20XX, Accepted Xth XXXXXXXXX 20XX

DOI: 10.1039/b000000x

A thermally-reversible inimer was used to confirm the controlled growth of individual branches during self-condensing vinyl atom transfer radical polymerization (ATRP). Segmented hyperbranched polymers were synthesized by ATRP of methyl methacrylate (MMA) and a novel inimer that contained a thermally labile Diels-Alder linkage between its initiating and polymerizable moieties. Three distinct feed ratios of MMA to inimer (15:1, 30:1, and 60:1) yielded hyperbranched polymers with variable degrees of branching and molecular weights in the range of 120,000 to 515,000 g/mol. The resulting hyperbranched polymers contained thermally-reversible branch points that were cleaved quantitatively on heating to yield linear polymers with molecular weights that were similar to the theoretical values that would be expected based on controlled chain growth of individual branches during self-condensing vinyl polymerization (SCVP). The cleaved linear polymers contained pendant furan and terminal maleimide functionalities that allowed reassembly at 50 °C to form "healed" hyperbranched polymers. The healing efficiency was determined by ^{1}H NMR spectroscopy, and the molecular weights of the repaired hyperbranched polymers were characterized by gel permeation chromatography. A segmented hyperbranched polymer was employed as a multifunctional macroinitiator to prepare an amphiphilic "hyper-star" *via* chain extension with poly(ethylene glycol) methyl ether methacrylate. Assembly of these "hyper-stars" into well-defined micelles (~23 nm) in neutral water was confirmed by transmission electron microscopy and dynamic light scattering.

Introduction

Segmented hyperbranched polymers,[1-6] a unique class of polymers with long linear chains between branch points, have received significant interest in polymer science. As compared to highly compact conventional hyperbranched polymers synthesized *via* AB_2 or $A_2 + B_3$ condensation polymerization,[7-11] the minimized steric hindrance between sparsely-branched backbones offers unique functionalization opportunities not available in more densely branched structures. In the last decade, self-condensing vinyl polymerization (SCVP)[12-20] has emerged as a robust method to prepare hyperbranched vinyl polymers. SCVP relies on the presence of a specific AB* monomer-initiator combination (*i.e.*, "inimer"). Inimers contain a polymerizable moiety capable of undergoing chain growth polymerization and an initiating moiety that can either (*i*) initiate new chains or (*ii*) condense with polymerizable groups present on other branched chains it encounters. Therefore, SCVP resembles both chain and step-growth polymerizations. Typically, polymers prepared by this method have broad molecular weight distributions and molecular weights that increase dramatically at high monomer conversion. The degree of branching achieved during SCVP can be tuned by including a conventional comonomer that is only capable of propagation. The resulting "segmented hyperbranched polymers" demonstrate interesting solution and melt properties as compared to their linear counterparts and contain a high density of functional groups at their periphery that can be used for subsequent addition of linear chains or functionalization with small molecules.

SCVP has been accomplished by a variety of controlled polymerization methods, including living ionic,[21] group transfer,[22-25] and controlled radical polymerization (CRP). Of particular interest are the well-established CRP methods: atom transfer radical polymerization (ATRP), [26-28] reversible addition-fragmentation chain transfer polymerization (RAFT),[29-33] and nitroxide-mediated polymerization (NMP).[34-36] For ATRP-based SCVP, the requisite inimer is a compound that contains a vinyl group for propagation and an activated halogen-containing group for initiation. Because of its well-known controlled polymerization characteristics, ATRP offers exceptional control over the architecture of segmented hyperbranched polymers prepared by SCVP and allows tuning of the linear chain length between branch points through careful modification of the ratio of inimer to comonomer in the feed.[37]

Assuming that each inimer incorporated into a growing chain during SCVP successfully undergoes initiation, the number and location of branch points in the chain is determined directly by the extent of inimer incorporation. In this case, each branch point would occur along the chain at the site at which the inimer is present. Therefore, we reasoned that incorporating a degradable linkage between the propagating and initiating groups of the inimer should lead to segmented hyperbranched polymers that can degrade into linear polymers upon cleavage of the labile linkage. Furthermore, we anticipated that including a reversible-covalent linkage in this site would produce a degradable

hyperbranched polymer capable of regenerating its original architecture upon cleavage and subsequent reconstruction. Reversible-covalent chemistries[38-40] have been utilized to prepare a variety of self-repairing polymers containing reversible covalent bonds. Compared to supramolecular interactions, [41] the enhanced strength of reversible covalent bonds offers the opportunity to achieve more stable structures while retaining the advantages of reversibility. To date, dynamic-covalent architectures such as block copolymers,[42] dendrimers,[43-44] stars,[45-47] polymeric networks,[48-55] and cyclic polymers[56-58] have been extensively investigated. Diels-Alder cycloadducts, imines, alkoxyamines, boronic esters, and disulfide linkages are among the moieties commonly exploited in the design of these versatile, functional architectures. Degradable segmented hyperbranched polymers have been prepared utilizing degradable inimers bearing disulfide,[16] ester[16] or acylal[59] groups. In response to changing pH or heat, these "smart" segmented hyperbranched polymers could be quantitatively cleaved to linear polymer chains. However, to the best of our knowledge, the reconstruction of degradable hyperbranched polymers has not been studied, which is likely due to the lack of suitable kinetics for esterification and acylal formation and the lack of selectivity during disulfide formation, the latter of which may lead to undesired gelation rather than the reconstruction of segmented hyperbranched architectures.

In our study, we present the synthesis of a novel, thermally-reversible ATRP inimer that contains a Diels-Alder linkage between its polymerizable and initiating groups. This inimer was copolymerized with methyl methacrylate (MMA) for the facile preparation of hyperbranched PMMA with predetermined linear segment lengths. Cleavage of the incorporated inimer units upon heating afforded linear PMMA copolymer fragments with narrow dispersity. The reconstruction of hyperbranched PMMA from cleaved linear PMMA was then examined. Additionally, the retained halogen atoms on the chain termini of the hyperbranched PMMA were used to initiate the polymerization of a water-soluble monomer to yield amphiphilic core-shell hyperbranched-linear copolymers (*i.e.*, "hyper-stars") through a grafting-from method.

Perhaps most significantly, we expected that the labile nature of the Diels-Alder inimer could be exploited to "reverse engineer" the segmented hyperbranched polymers to determine the extent to which individual branches grew in the controlled manner expected for ATRP. While SCVP is expected to cause non-linear evolutions of molecular weight with conversion and to generate branched polymers with broad molecular weight distributions,[60] the control afforded by ATRP is assumed to mediate the growth of individual branches. In this study, we triggered the degradation of these segmented hyperbranched copolymers to allow the detailed analysis of their individual linear components. Therefore, the reversibility of the Diels-Alder inimer yielded adaptive/responsive materials while also providing fundamental insight into the mechanism of a widely utilized method of branched polymer synthesis.

Results and Discussion

Preparation of thermally reversible Diels-Alder inimer. Our goal was to prepare segmented hyperbranched polymers capable of dissociating into their individual linear components and undergoing repair during a subsequent reconstruction process. To accomplish this, we synthesized a novel inimer that contained a Diels-Alder adduct between its polymerizable and initiating fragments with the expectation that heating to a temperature which favored the retro-Diels-Alder reaction would lead to cleavage of the branched structure to yield linear polymers. Successful synthesis of the precursor and Diels-Alder inimer were confirmed by ^{1}H and ^{13}C NMR spectroscopy (Figure 1 and Figure S1). The combination of extended reaction times (48 h) and relatively high temperatures (75 °C) during the synthesis of the inimer precursor favored the near-quantitative formation of the more thermodynamically stable *exo* cycloadduct.

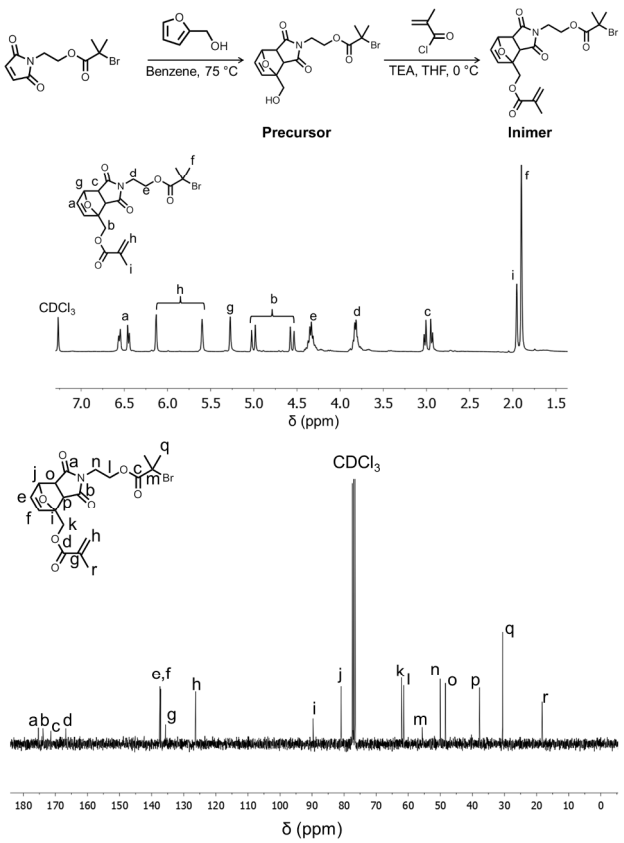

Figure 1. Synthesis, ^{1}H and ^{13}C NMR spectra of the Diels-Alder inimer.

Synthesis and Characterization of Segmented Hyperbranched PMMA. Copolymerization of the Diels-Alder inimer with MMA afforded branched PMMA with degrees of branching (DB) that should depend on the [MMA]:[inimer] ratio.[60] To determine the temperature at which the polymerizations could be conducted, the thermal stability of the inimer was investigated. No change in the NMR spectra of the inimer was observed after 24 h at 45 °C,

suggesting that the retro-Diels-Alder reaction did not occur to an appreciable extent under these conditions. Therefore, 45 °C was chosen as the polymerization temperature for the SCVP of MMA and the newly designed inimer.

To discern the influence of the [monomer]:[CuBr] ratio, two different ratios (40:1 and 100:1) were applied to the copolymerization of MMA and inimer, keeping the initial monomer concentration at a constant value of 5 M in toluene. Table 1 presents the results of these experiments. The overall conversions of vinyl groups rapidly approached 99% within 4 h at a lower monomer to catalyst ratio (40:1). However, at 100:1 ratio of monomer to catalyst, the monomer conversion only reached 80% after 20 h, indicating a slower polymerization process than those conducted with higher catalyst loading. Furthermore, the molecular weight and M_w/M_n of the resulting polymers at the lower monomer to catalyst ratio (40:1) were significantly larger than those at a higher monomer to catalyst ratio (100:1). These results suggest increased condensation between branched macromolecules at higher monomer conversions,[37] resulting in a sizable increase in polymer molecular weight and broadening of the molecular weight distribution. This phenomenon is in accordance with the inherent nature of SCVP.

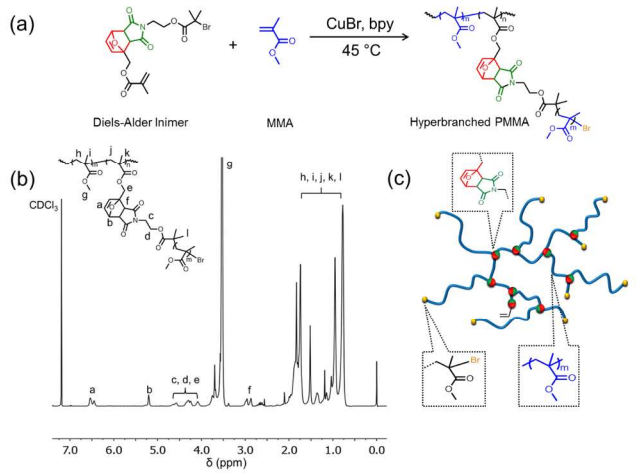

Figure 2. (a) General protocol for the preparation of segmented hyperbranched PMMA by SCVP**; (b)** ^{1}H NMR of **SHB P2** (see Table 1); **(c)** Representation of segmented hyperbranched PMMA.

Notably, at monomer to catalyst ratio of 100:1, the conversion only reached 80% after extended reaction times and did not increase significantly after 20 h. This result suggests the catalyst efficiency was diminished, potentially due to the persistent radical effect (PRE) common for methacrylate type ATRP inimers.[61] The high ATRP equilibrium constant of 2-haloisobutyrates results in irreversible conversion of activating Cu(I)Br to deactivating Cu(II)Br_2. The accumulation of Cu(II)Br_2 shifts the equilibrium towards the dormant species, reducing the concentration of propagating radicals. Therefore, in the application of SCVP of MMA, a sufficient catalyst loading or addition of a reducing agent (*e.g.*, Cu(0)) is necessary to overcome the PRE and to reach high conversion.[16,62]

Given that 40:1 was determined as a satisfactory value of monomer to catalyst ratio, three segmented hyperbranched PMMA (**SHB P1**, **SHB P2**, and **SHB P3**) with linear segments between branches of varying lengths were synthesized under these conditions (Table 1). Their structures were confirmed by ^{1}H NMR spectroscopy (Figure 2). As shown in Table 1, molecular weights determined by GPC at 99% conversion increased with the initial feed ratio of monomer to inimer, in accordance with previous reports.[59,63] The values of the absolute M_w determined for each branched polymer from GPC−MALLS were significantly higher than the corresponding apparent molecular weights determined by conventional calibration with PMMA standards. This well-known phenomenon stems from the compact, globular structure of the hyperbranched polymers as compared to the linear calibration standards.

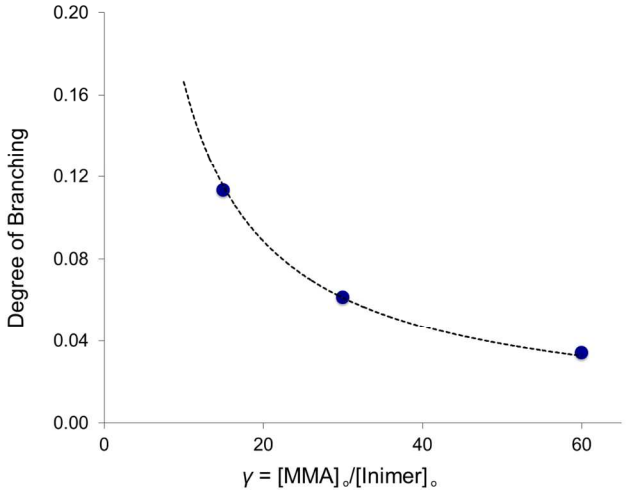

Figure 3. Degree of branching (DB) as a function of feed ratio at full monomer conversion (blue circles represent DB values obtained from ^{1}H NMR spectroscopy; dotted line represents theoretically derived DB values)

With the assumption that the number of terminal bromide units is equal to the number of branch points[15], Equation 1 was used to estimate the degree of branching for **SHB P1-P3**, where A_b and A_g correspond to the ^{1}H NMR spectroscopy peak integrations for protons *b* and *g*, respectively, as labeled in Figure 2.[60]

$$DB = \frac{2A_b}{2A_b + \frac{A_g}{3}} \qquad (1)$$

We observed excellent agreement between the theoretical and experimentally determined DB values obtained at full monomer conversion (>99%) at all $\gamma = [MMA]_o:[Inimer]_o$ ratios (Figure 3) As expected, a higher content of inimer (lower γ) resulted in higher DB, consistent with values obtained from the theoretical equation proposed by Müller *et al.*[60]

Polymerization Kinetics of ATRP-SCVP of MMA/Inimer. As the discussion above indicates, the commonly accepted mechanism of SCVP would predict that the length of linear

PMMA between branches can be controlled by the feed ratio (and relative reactivities) of MMA and inimer. While the evolution of molecular weight with conversion is expected to be non-linear as a result of the combined step/chain-growth mechanisms of SCVP, each individual arm of the branched polymer should grow in a manner predicted by the general ATRP process. The presence of degradable linkages at each branched point allowed us to cleave the branched polymers to yield their linear components. We reasoned that analysis of the resulting linear polymers would provide insight into the control achieved during the growth of each individual arm.

To further understand the SCVP process as applied to the synthesis of segmented hyperbranched polymers and to investigate the regularity of the linear segments that result, kinetic studies were conducted with an initial monomer to inimer ratio of 60:1 under the aforementioned optimized reaction conditions. At predetermined time points, aliquots were taken from the SCVP reaction solution. The aliquots were divided with one portion being immediately used for both ^{1}H NMR spectroscopy and GPC analysis to obtain information on the intact hyperbranched PMMA. The remaining solution was precipitated into cold methanol to remove residual monomer, and the resulting polymer was dried, redissolved in toluene, and subjected to heating at 120 °C to completely cleave the polymer at its branch points by a retro-Diels-Alder reaction. After 1 h, the reactions were quenched by immersion in liquid nitrogen, and the degraded linear PMMA samples were characterized by GPC.

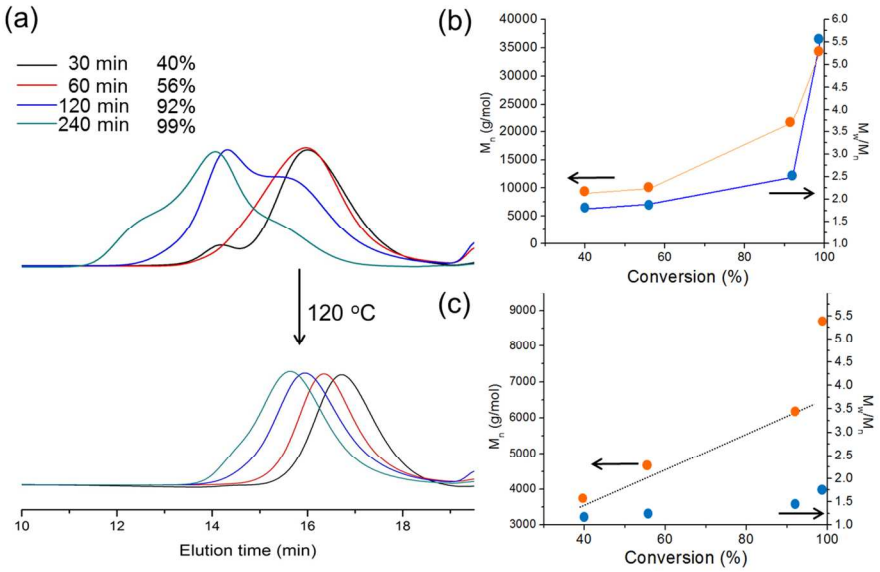

Figure 4. (a) GPC traces as a function of conversion during the SCVP of MMA[a] (top) and the corresponding cleaved linear PMMA after the retro-Diels-Alder reaction at 120 °C (bottom); (b) M_n and M_w/M_n of hyperbranched PMMA as a function of monomer conversion during the SCVP of MMA; (c) M_n and M_w/M_n of the corresponding cleaved linear PMMA as a function of monomer conversion (dotted line represents theoretical M_n). [a]([MMA]$_o$ + [Inimer]$_o$):[CuBr]$_o$:[bpy]$_o$ = 40:1:2 at 45 °C, [MMA]$_o$ = 5 M, [MMA]$_o$:[Inimer]$_o$ = 60:1.

Table 1. Hyperbranched polymers prepared from *via* SCVP of inimer and MMA

				GPC		GPC-MALLS
Entry	Feed ratio[c]	Time (h)	Conversion (%)	M_n (g/mol)	M_w/M_n	M_w (g/mol)
SHB P1[a]	15	4	99	11 000	3.62	120 000
SHB P2[a]	30	3	99	17 000	4.95	260 000
SHB P3[a]	60	4	99	36 300	5.37	515 000
SHB P4[b]	30	20	75	8 800	2.33	23 400
SHB P5[b]	60	20	80	10 700	1.83	33 100

[a]([MMA]$_o$ + [Inimer]$_o$):[CuBr]:[bpy]$_o$ = 40:1:2, [MMA]$_o$ = 5 M. [b]([MMA]$_o$ + [Inimer]$_o$):[CuBr]:[bpy]$_o$ = 100:1:2, [MMA]$_o$ = 5M. [c]Feed ratio represents initial molar ratio of MMA to inimer.

The results of this kinetic study are summarized in Table 2. As shown in Figure 4a and 4b, the molecular weight and M_w/M_n of the intact hyperbranched PMMA grew as a function of time and conversion as expected. At high conversion, a substantial increase in molecular weight of hyperbranched polymers was observed from 29,400 (92%) to 118,400 (99%). Broad molecular weight distributions were observed, with significant multimodality developing as the polymerization proceeds. These observations are consistent with the expected behavior of SCVP and is likely due to the rate of condensation between macromolecules being dependent on the number of end groups on each branched macromolecule. Larger macromolecules contain more halogen end groups that can be activated to add monomer and condense with other branched molecules, leading to higher molecular weight polymers growing faster than low molecular ones. However, analysis of the samples that resulted after cleavage of the hyperbranched polymers yielded results that were indicative of linear polymers with narrow molecular weight distributions. Additionally, across most of the conversion range, the increase in M_n followed the theoretical prediction calculated from [MMA]:[inimer] ratios and conversion. Furthermore, the M_w/M_n of segments remain relatively low (<1.4) up to high monomer conversion (Table 2 and Figure 4c). These important results suggest the individual branches of polymers made by SCVP grow in a controlled manner, similar to that expected for ATRP with more conventional (*i.e.*, non-inimer) alkyl halide initiators. At very high conversions (>99%), a small high molecular shoulder on the GPC traces of the linear polymer was observed, and there was deviation from the theoretical molecular weight. This observation could result from the highly congested environment of the propagating chain ends late in the polymerization leading to increased intramolecular chain coupling. Just as an increased contribution from termination reactions can be observed at high conversion during conventional ATRP, the same may occur in this case, especially given the high local concentration of chain ends in hyperbranched systems. At high catalyst loadings (40:1), more extensive activation and faster propagation compromised the amount of control normally afforded by ATRP. It is expected that better precision could be achieved by employing lower catalyst concentrations, however, in the case of SCVP, this would lead to a dramatic reduction in monomer conversion and degree of branching. It should also be noted that the similar reactivities of monomer and inimer vinyl groups in this particular system enhances the regulation of chain growth during SCVP.[2]

Table 2. Preparation of segmented hyperbranched MMA copolymers (**SHB P3**) and their thermal degradation products (120 °C for 1 h)[a]

			Before thermal degradation			After thermal degradation		
Entry	Time (h)	Conv. (%)	M_n (g/mol)[b]	M_w/M_n[b]	M_n (g/mol)[c]	$M_{n,theo}$ (g/mol)[d]	M_n (g/mol)[b]	M_w/M_n[b]
1	0.5	40	6 300	2.13	12 500	2 860	3 300	1.13
2	1.0	56	7 100	2.24	15 600	3 830	4 150	1.22
3	2.0	92	11 900	3.71	29 400	5 970	6 100	1.41
4	4.0	99	36 300	5.37	118 400	6 400	8 700	1.73

[a] $([MMA]_o + [Inimer]_o):[CuBr]_o:[bpy]_o = 40:1:2$, $[MMA]_o = 5$ M, $[MMA]_o:[Inimer]_o = 60:1$.
[b] Determined by GPC with PMMA standards. [c] Determined by GPC-MALLS.
[d] $M_{n,\,theo} = [MMA]_o/[Inimer]_o \times \text{conversion} \times MW_{monomer} + MW_{inimer}$

Extension of PEGMA from hyperbranched PMMA. The ability for chain extension from hyperbranched polymers is intriguing in regards to the preparation of more complex architectures. To confirm the retention of terminal bromide (Br) atoms on the hyperbranched polymers, **SHB P2** was used as a multifunctional macroinitiator and was chain extended with PEGMA (60:1 PEGMA:Br; Scheme 1) to yield core-shell copolymers with branched PMMA cores and linear poly(PEGMA) (PPEGMA) shells. After 7 h (34% conversion), the reaction was stopped, and the structure of the "hyper-star" copolymer was verified by ^{1}H NMR spectroscopy (Figure S2), which indicated peaks characteristic of both PMMA and PPEGMA. GPC revealed a reduction in the retention time, indicative of an increase in molecular weight during extension (Figure 5). Unlike the original PMMA-based starting material, the amphiphilic hyper-star could be dispersed in water (a selective solvent for the PPEGMA shell). Aqueous solutions of these materials were further characterized by dynamic light scattering (DLS) and transmission electron microscopy (TEM) (Figure 6). DLS offered evidence of self-assembled particles with a hydrodynamic diameter (D_h) of 23 nm in neutral water, which was in good agreement with TEM results (21 nm in diameter). Notably, the hydrodynamic diameter of the hyper-star in toluene (a non-selective solvent) was only 7 nm, which is a size consistent with that of molecularly dissolved unimers (Figure 6c). Therefore, it seems reasonable that dissolution in water leads to assembly of individual hyper-stars into micellar structures in which an aggregated hydrophobic PMMA core is stabilized by a water-soluble PPEGMA corona. The formation of larger nanostructures suggests the core of **SHB P2** must be sparsely branched to the degree that intermolecular interactions between hyper-star macromolecules are possible (Figure 6a).

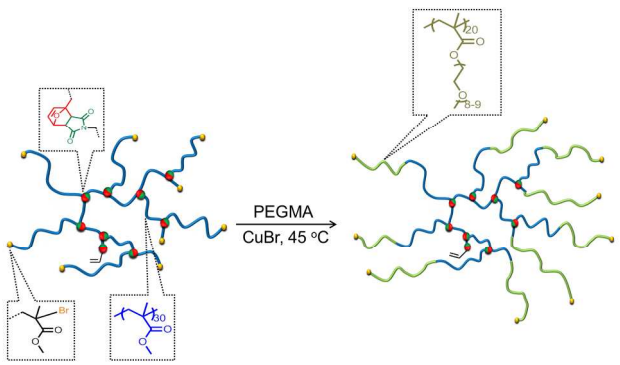

Scheme 1. Chain extension of segmented hyperbranched PMMA (**SHB P2**) with PEGMA.

The hyper-star was thermally treated at 120 °C in toluene for 1 h. A shift to longer retention time was observed by GPC analysis, indicative of degradation and reduced molecular weight during the retro-Diels-Alder reaction (Figure S3a). The results suggest the formation of linear block copolymer $PMMA_{30}$-*b*-$PPEGMA_{20}$, with a higher molecular weight than the corresponding cleaved $PMMA_{30}$ homopolymer (Figure S3b). The polydispersity of the resultant block copolymers remained as low as M_w/M_n = 1.42, suggesting some degree of control during the chain extension from the **SHB P2** core. The lack of a low molecular weight shoulder in the chromatogram reinforces this point, along with providing evidence of high initiation efficiency from the macroinitiator. Therefore, even at high monomer conversion, a significant number of terminal bromide atoms are retained during the preparation of hyperbranched PMMA, which further corroborates the controlled nature of the original SCVP.

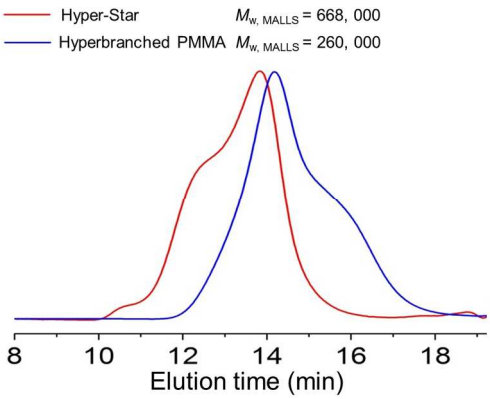

Figure 5. GPC traces before and after chain extension of **SHB P2** with PEGMA.

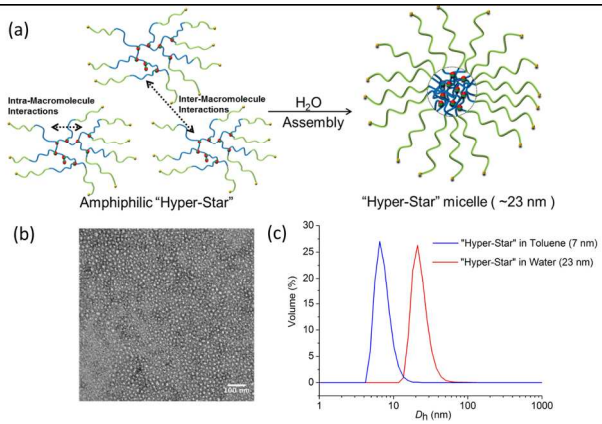

Figure 6. (a) Proposed self-assembly of hyper-stars in water; (b) TEM of hyper-star based micelles cast from aqueous solution; (c) DLS size distributions of the hyper-stars in water (selective solvent) and toluene (non-selective solvent).

Thermal degradation of segmented hyperbranched PMMA. Degradation of the hyperbranched PMMA was studied in more detail to gain insight into the efficiency and kinetics of the thermally driven retro-Diels-Alder reaction. The degradation of **SHB P1-P5** was carried out under heating at 90 or 120 °C. The results are summarized in Table S1. ^{1}H NMR spectroscopy was employed to observe the degradation process (Figure S4b). After 1 h at 120 °C, complete disappearance of the signals associated with the Diels-Alder adduct was observed, while the signals from the pendant furan and terminal maleimide groups became apparent. This observation is consistent with quantitative cleavage of branching points to result in linear segments. Accordingly, a shift of the GPC chromatograms to longer retention times occurred within 1 h, with no further differences being observed after extended thermal treatment (Figure S4c). These results indicate the retro-Diels-Alder degradation process is rapid and highly efficient at 120 °C.

At the lower temperature of 90 °C, the reversion reaction was significantly slower, which facilitated monitoring the kinetics of the degradation process (Figure 7a). The degradation of **SHB P1** into its linear segments at 90 °C was monitored by ^{1}H NMR spectroscopy and GPC (Figure 7b and 7c). GPC traces for samples taken at various extents of reaction during the degradation of **SHB P1** at 90 °C offered evidence of degradation, as the molecular weight distributions became more narrow and unimodal and the average molecular weight decreased with time (Figure 7b). Moreover, it was particularly interesting that the progress of the retro-Diels-Alder reaction, as determined by ^{1}H NMR spectroscopy, was directly coupled to the reduction in molecular weight determined by GPC (Figure 7c). The degradation reaction reached a maximum conversion of ~80% after 15 h, after which the equilibrium between cycloaddition and cycloreversion was established with no further reaction being observed.

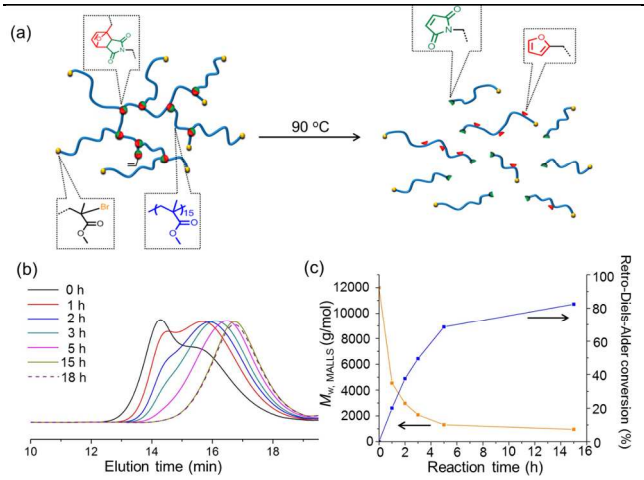

Figure 7. (a) Degradation of segmented hyperbranched polymers at 90 °C; (b) GPC traces of samples taken during thermal degradation of **SHB P1** at 90 °C; (c) Evolution of absolute M_w determined by MALLS and retro-Diels-Alder conversion as a function of reaction time.

Thermal reformation of segmented hyperbranched PMMA. Diels-Alder chemistry has been widely employed in the area of self-healing materials due to its frequent classification as a "click" reaction[64] and its facile reversibility. Taking advantage of these properties, our novel inimer-based hyperbranched polymers were expected to exhibit self-repairing behavior on the molecular scale similar to other Diels-Alder-based bulk polymeric materials.[65]

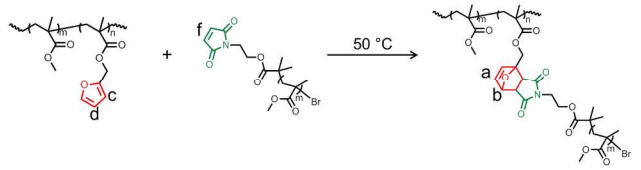

Scheme 2. Repair of hyperbranched PMMA *via* Diels-Alder cycloaddition of linear PMMA.

Thermal reassembly of **SHB P1-P3** was investigated by ^{1}H NMR spectroscopy using the corresponding cleaved linear polymers (**L P1**, **L P2** and **L P3,** Table 3). The linear polymers were allowed to recombine at 50 °C in toluene (Scheme 2). At the onset of the reaction of **L P1**, no Diels-Alder cycloadduct peaks were observed. As the polymer solution was heated, the Diels-Alder reaction between furan and maleimide proceeded, as evidenced by the gradual growth of the cycloadduct peaks at 5.2-5.3 ppm, coinciding with the decrease of maleimide peaks at 6.7 ppm (Figure 8b). After 24 h of heating, 70% of maleimide groups were consumed. However, an additional 24 h of heating only resulted in a 3% increase in conversion, suggesting that equilibrium had been established. Notably, the pattern of cycloadduct signal at 5.2-5.3 ppm slowly shifts from 5.25 ppm to 5.20 ppm, indicating the formation of the favored *exo* isomer over an extended period of heating. Furthermore, the Diels-Alder cycloaddition efficiency was also tested for **L P2** and **L P3** (Figure 8a). Interestingly, the efficiency of repair was decreased with increasing linear segment length, which is likely due to the increased steric hindrance that limits the ability of terminal maleimide and pendant furan groups on long chains to recombine. Additionally, the concentration of functionality on the polymers decreases as the length of linear segments increases, resulting in lower Diels-Alder reaction rates. Incomplete repair was also confirmed by comparing the DB of the polymers (**SHB P1-P3**) before degradation and after repair using Equation 1. It was clearly observed that increased segment length (*i.e.,* higher feed ratio of monomer to inimer) led to diminished recovery of degree of branching in the healed polymers (Table 3, Figure 10).

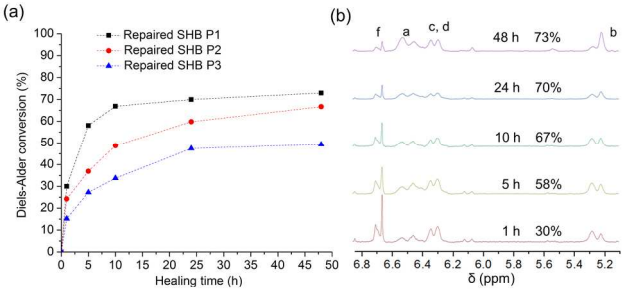

Figure 8. (a) Reconstruction kinetics of **SHB P1-P3** as quantified by ^{1}H NMR spectroscopy; (b) ^{1}H NMR spectra of **SHB P1** during repair at 50 °C. Peak assignments correspond to the proton labels in Scheme 2.

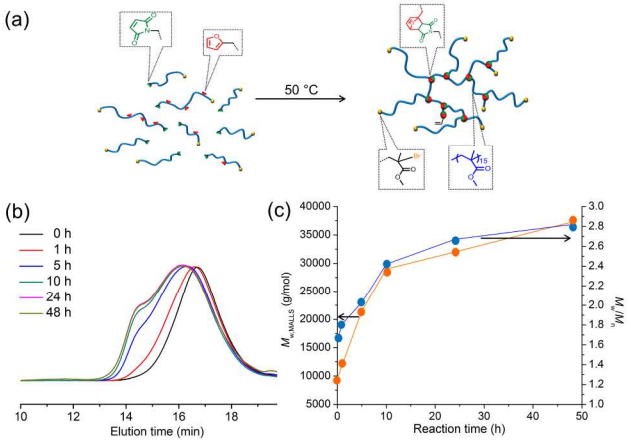

Figure 9. (a) Reconstruction of segmented hyperbranched PMMA at 50 °C; (b) GPC traces of reformed **SHB P1** as a function of time during thermal treatment at 50 °C; (c) Evolution of $M_{w,MALLS}$ and M_w/M_n of repaired **SHB P1** as a function of time.

The evolution of molecular weight during the healing reaction was also investigated. As the duration of thermal treatment increased, both the absolute M_w and M_w/M_n of **SHB P1** became larger, indicating successful repair of the hyperbranched polymers (Figure 9). Although the conversion of the repair reaction reached 73% after 48 h, the ultimate absolute M_w of the reconstructed hyperbranched polymer was significantly lower

Table 3. Results from repair of the hyperbranched polymers after heating solutions of the degraded linear polymers at 50 °C for 48 h

	Before thermo-healing		After thermo-healing				
	GPC		GPC		GPC-MALLS		
Entry	M_n (g/mol)	M_w/M_n	M_n (g/mol)	M_w/M_n	M_w (g/mol)	Healing efficiency[a]	DB Recovery[b]
L P1[a]	3 500	1.65	6 400	3.03	37 300	73%	75%
L P2[a]	5 600	1.78	9 200	3.13	52 100	65%	70%
L P3[a]	8 700	1.73	12 000	2.36	39 600	48%	39%

[a]From ^{1}H NMR spectroscopy of cycloadduct protons; [b]From ^{1}H NMR spectroscopy and Equation 1

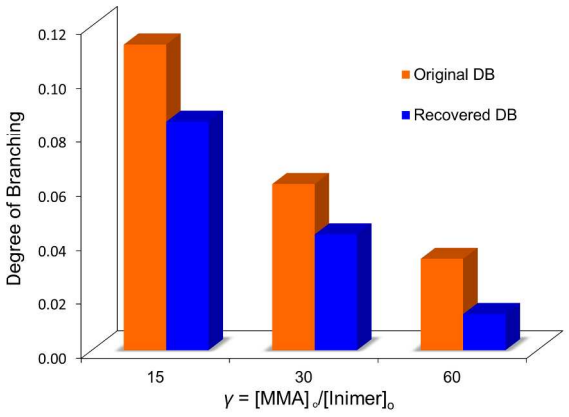

Figure 10. DB of original segmented hyperbranched polymers and reconstructed hyperbranched polymers.

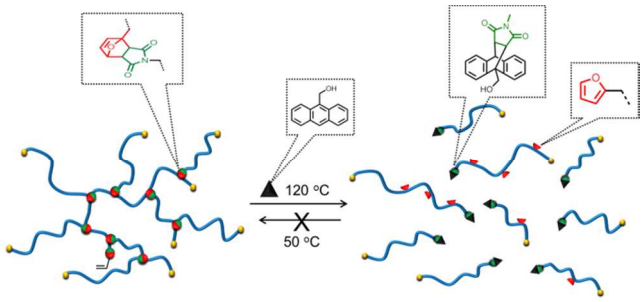

Scheme 3. In-situ retro-Diels-Alder reaction of furan-maleimide based DA bond and formation of anthracene-maleimide linkage at 120 °C.

than that of the original **SHB P1** (37,300 *vs.* 120,000 g/mol, Table 1 and Table 3). This result again suggests the efficiency of reconstruction process is limited due to the steric hindrance associated with the condensation of linear polymers to reform the densely-packed, hyperbranched polymer. In some ways, this phenomenon is similar to the reduced efficiency observed during "grafting-to" type reactions of other polymer systems.[66] Low functional group concentration and steric hindrance limits the efficiency of the polymer-polymer reactions required during healing, while the original hyperbranched polymer was formed under SCVP conditions that more closely approximated those of a "grafting-from" process in which low molecular weight monomers reacted with growing chains under less sterically demanding conditions.

Mechanism of degradation and reconstruction. To unequivocally demonstrate degradation and reconstruction occurred via Diels-Alder cycloreversion and cycloaddition, respectively, two model reactions were conducted. The first reaction involved quenching the reactive maleimides that should be produced during the retro-Diels-Alder degradation process such that subsequent repair would become impossible (Scheme 3). Therefore, the repair of hyperbranched PMMA was attempted in the presence of a large excess of a thermally stable dienophile trapping agent. **SHB P4** was cleaved at 120 °C in the presence of 9-anthracenemethanol. While this temperature favors cycloreversion for furan-maleimide Diels-Alder adducts, it favors cycloaddition for anthracenes and maleimides. Therefore, the maleimide groups that result from thermal degradation of the hyperbranches should be scavenged by the excess functional anthracene. The resulting "quenched" linear polymers were then held at 50 °C and characterized by GPC as a function of time. As expected, the traces of the "repaired" **SHB P4** did not shift to higher molecular weight (Figure S5). The absence of reformation under these conditions confirms that the healing mechanism is centered on the furan-maleimide based Diels-Alder reaction.

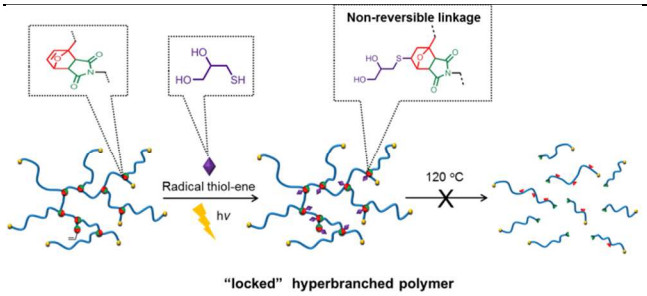

Scheme 4. Thiol-ene reaction between 1-thioglycerol and segmented hyperbranched PMMA.

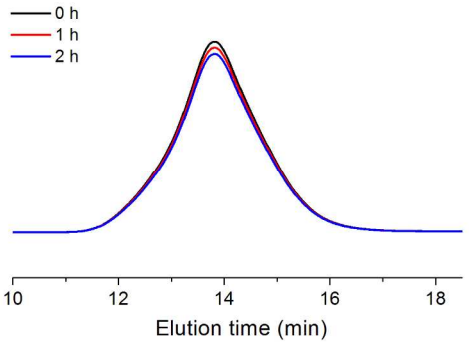

Figure 11. GPC traces of samples taken during thermal treatment of "locked" **SHB P2** at 120 °C. No change in molecular weight was observed due to the loss of the oxy-norbornene group during the preceding thiol-ene reaction.

The second model reaction involved "locking" of the inimer units within the hyperbranched polymers by the addition of a small molecule thiol to the double bond of the substituted cyclohexene Diels-Alder adduct (Scheme 4). This reaction was expected to consume the double bond required for cycloreversion.[67,68] The oxy-norbornene functional group is susceptible to transformation *via* thiol-ene chemistry, in which thiols add irreversibly across alkenes under UV irradiation. Consumption of the vinyl groups in Diels-Alder-linked segmented hyperbranched polymers by 1-thioglycerol prohibited cycloreversion reactions, eliminating degradation of the polymers. After irradiation (365 nm, 100 W, 100 min), ^{1}H NMR revealed quantitative consumption of the oxy-norbornene protons (*a*, 6.5 ppm) and –C***H***O– bridge-head protons (*b*, 5.23 ppm), while new signals corresponding to –C***H***O– protons (*d*, 4.8 ppm) and saturated methylene protons (*c*, 2.1 ppm) were also observed (Figure S6). The thiol-locked **SHB P2** was subjected to heating at 120 °C in toluene and the reaction was monitored by GPC (Figure 11). As expected, the locked polymers did not degrade when heated, further supporting that the degradation mechanism occurs *via* the furan-maleimide based retro-DA reaction at the branch points. Not only does this model reaction help support the proposed Diels-Alder cycloreversion process, it also provides a means by which otherwise thermally-labile hyperbranches can be rendered stable. Additionally, this thiol-ene based approach may be utilized to attach desired functionalities at branch points within segmented hyperbranched polymers in a modular manner, further extending their versatility and potential applications.

Conclusions

In summary, novel hydrophobic and amphiphilic dynamic-covalent macromolecular assemblies have been successfully prepared by ATRP-SCVP. Hyperbranched copolymers with thermally-labile furan-maleimide Diels-Alder adduct branch points were readily cleaved at high temperatures and repaired at lower temperatures. This method extends the concept of self-repair from the materials level to the macromolecular scale. Perhaps most importantly, the ease with which the hyperbranched polymers could be efficiently degraded allowed us to examine the resulting linear polymer products to gain insight into the control achieved during the growth of individual branches by SCVP. It was determined that while the growth in molecular weight during the copolymerization of an inimer with another comonomer occurs in a complex manner, the growth of individual branches proceeds by a controlled polymerization process that is consistent with ATRP.

Notes and references

George & Josephine Butler Polymer Research Laboratory, Center for Macromolecular Science & Engineering, Department of Chemistry, University of Florida, PO Box 117200, Gainesville, FL 32611-7200, USA. E-mail: sumerlin@chem.ufl.edu; Fax: +1 352 392 9741

This material is based upon work supported by the National Science Foundation (DMR-1410223).

† Electronic Supplementary Information (ESI) available: [details of any supplementary information available should be included here]. See DOI: 10.1039/b000000x/

1. S. Muthukrishnan, D. P. Erhard, H. Mori and A. H. E. Müller, *Macromolecules*, 2006, **39**, 2743.
2. J. Han, S. Li, A. Tang and C. Gao, *Macromolecules*, 2012, **45**, 4966.
3. D. Konkolewicz, C. K. Poon, A. Gray-Weals and S. Perrier, *Chem. Commun*., 2011, **47**, 239.
4. N. Clarke, E. de Luca, J. M. Dodds, S. M. Kimani and L. R. Hutchings, *Eur. Polym. J*., 2008, **44**, 665.
5. A. Pfaff and A. H. E. Müller, *Macromolecules*, 2011, **44**, 1266.
6. S. Li, J. Han and C. Gao, *Polym. Chem*., 2013, **4**, 1774.
7. M. Calderón, M. A. Quadir, S. K. Sharma and R. Haag, *Adv. Mater*., 2010, **22**, 190.
8. M. Jikei and M. Kakimoto, *Prog. Polym. Sci*., 2001, **26**, 1233.
9. C. Gao and D. Yan, *Prog. Polym. Sci*., 2004, **29**, 183.
10. C. M. Paleos, D. Tsiourvas and Z. Sideratou, *Mol. Pharm*., 2007, **4**, 169.
11. X. Yu, Z. Liu, J. Janzen, I. Chafeeva, S. Horte, W. Chen, R. K. Kainthan, J. N. Kizhakkedathu and D. E. Brooks, *Nat. Mater*., 2012, **11**, 468.
12. (a) A. P. Vogt and B. S. Sumerlin, *Macromolecules*, 2008, **41**, 7368; (b) A. P. Vogt, S. R. Gondi and B. S. Sumerlin, *Australian Journal of Chemistry*, 2007, **60**, 396.
13. (a) C. Cheng, K. L. Wooley and E. Khoshdel, *J. Polym. Sci*., Part A: Polym. Chem., 2005, **43**, 4754; (b) R. M. England and S. Rimmer, *Polym. Chem*., 2010, **1**, 1533.
14. S. Muthukrishnan, H. Mori and A. H. E. Müller, *Macromolecules*, 2005, **38**, 3108.

15. K. Min and H. Gao, *J. Am. Chem. Soc*., 2012, **134**, 15680.
16. N. V. Tsarevsky, J. Huang and K. Matyjaszewski, *J. Polym. Sci., Part A: Polym. Chem*., 2009, **47**, 6839.
17. C. J. Hawker, J. M. J. Frechet, R. B. Grubbs and J. Dao, *J. Am. Chem. Soc*., 1995, **117**, 10763.
18. A. V. Ambade and A. Kumar, *Prog. Polym. Sci*., 2000, **25**, 1141.
19. R. Baudry and D. C. Sherrington, *Macromolecules*, 2006, **39**, 1455.
20. R. Baudry and D. C. Sherrington, *Macromolecules*, 2006, **39**, 5230.
21. J. M. J. Frechet, M. Henmi, I. Gitsov, S. Aoshima, M. R. Leduc and R. B. Grubbs, *Science*, 1995, **269**, 1080.
22. V. Bütün, I. Bannister, N. C. Billingham, D. C. Sherrington and S. P. Armes, *Macromolecules*, 2005, **38**, 4977.
23. P. F. W. Simon, W. Radke and A. H. E. Müller, *Macromol. Rapid Commun*., 1997, **18**, 865.
24. P. F. W. Simon, A. H. E. Müller and T. Pakula, *Macromolecules*, 2001, **34**, 1677.
25. P. F. W. Simon and A. H. E. Müller, *Macromolecules*, 2001, **34**, 6206.
26. S. G. Gaynor, S. Edelman and K. Matyjaszewski, *Macromolecules*, 1996, **29**, 1079.
27. K. Matyjaszewski, S. G. Gaynor, A. Kulfan and M. Podwika, *Macromolecules*, 1997, **30**, 5192.
28. (a) P. M. Imbesi, J. A. Finlay, N. Aldred, M. J. Eller, S. E. Felder, K. A. Pollack, A. T. Lonnecker, J. E. Raymond, M. E. Mackay, E. A. Schweikert, A. S. Clare, J. A. Callow, M. E. Callow and K. L. Wooley, *Polym. Chem*., 2012, **3**, 3121; (b) V. Percec, B. Barboiu, C. Grigoras and T. K. Bera, *J. Am. Chem. Soc*., 2003, **125**, 6503; (c) C. Lu, Q. Liu, P. Gu, D. Chen, F. Zhou, H. Li and Q. Xu, *Polym. Chem*., 2014, **5**, 2602.
29. S. Carter, B. Hunt and S. Rimmer, *Macromolecules*, 2005, **38**, 4595.
30. S. Rimmer, S. R. Carter, and R. Rutkaite, J. W. Haycock and L. Swanson, *Soft Matter*, 2007, **3**, 971.
31. S. R. Carter, R. M. England, B. Hunt and S. Rimmer, *Macromol. Biosci*., 2007, **7**, 975.
32. (a) J. Schmitt, N. Blanchard and J. Poly, *Polym. Chem*., 2011, **2**, 2231; (b) F. Isaure, P. A. G. Cormack and D. C. Sherrington, *Macromolecules*, 2004, **37**, 2096.
33. Z. Wang, J. He, Y. Tao, L. Yang, H. Jiang and H. Y. Yang, *Macromolecules*, 2003, **36**, 7446.
34. C. Li, J. He, L. Li, J. Cao and Y. Yang, *Macromolecules*, 1999, **32**, 7012.
35. A. Niu, C, Li, Y. Zhao, J. He, Y. Yang and C. Wu, *Macromolecules*, 2001, **34**, 460.
36. Y. Tao, J. He, Z. Wang, J. Pan, H. Jiang, S. Chen and Y. Yang, *Macromolecules*, 2001, **34**, 4742.
37. F. Bally, E. Ismailova, C. Brochon, C. A. Serra and G. Hadziioannou, *Macromolecules*, 2011, **44**, 7124.
38. J.-M. Lehn, *Chem.–Eur. J*., 1999, **5**, 2455.
39. P. T. Corbett, J. Leclaire, L. Vial, K. R. West, J.-L. Wietor, J. K. M. Sanders and S. Otto, *Chem. Rev*., 2006, **106**, 3652.
40. S. J. Rowan, S. J. Cantrill, G. R. L. Cousins, J. K. M. Sanders and J. F. Stoddart, *Angew. Chem. Int. Ed*., 2002, **41**, 898.
41. *Supramolecular Polymers*, ed. A. Ciferri, CRC Press, 2005.
42. J. A. Syrett, G. Mantovani, W. R. S. Barton, D. Price and D. M. Haddleton, *Polym. Chem*., 2010, **1**, 102.
43. J. R. McElhanon and D. R. Wheeler, *Org. Lett*., 2001, **3**, 2681.
44. M. L. Szalai, D. V. McGrath, D. R. Wheeler, T. Zifer and J. R. McElhanon, *Macromolecules*, 2007, **40**, 818.
45. A. P. Bapat, J. G. Ray, D. A. Savin, E. A. Hoff, D. L. Patton and B. S. Sumerlin, *Polym. Chem*., 2012, **3**, 3112.
46. A. P. Bapat, D. Roy, J. G. Ray, D. A. Savin and B. S. Sumerlin, *J. Am. Chem. Soc*., 2011, **133**, 19832.
47. A. P. Bapat, J. G. Ray, D. A. Savin and B. S. Sumerlin, *Macromolecules*, 2013, **46**, 2188.
48. P. Reutenauer, E. Buhler, P. J. Boul, S. J. Candau and J.-M. Lehn, *Chem. Eur. J*., 2009, **15**, 1893.
49. Y. Amamoto, J. Kamada, H. Otsuka, A. Takahara and K. Matyjaszewski, *Angew. Chem. Int. Ed*., 2011, **123**, 1698.
50. A. J. Inglis, L. Nebhani, O. Altintas and C. Barner-Kowollik, *Macromolecules*, 2010, **43**, 5515.
51. T. Ono, T. Nobori and J.-M. Lehn, *Chem. Commun*., 2005, 1522.
52. R. K. Schultz and R. R. Myers, *Macromolecules*, 1969, **2**, 281.
53. Y. Chujo, K. Sada, R. Nomura, A. Naka and T. Saegusa, *Macromolecules*, 1993, **26**, 5611.
54. A. P. Vogt and B. S. Sumerlin, *Soft Matter*, 2009, **5**, 2347.
55. M. Nakahata, Y. Takashima, H. Yamaguchi and A. Harada, *Nat. Commun*., 2011, **2**, 511.
56. S. Ulrich, E. Buhler and J.-M. Lehn, *New J. Chem*., 2009, **33**, 271.
57. G. Yamaguchi, Y. Higaki, H. Otsuka and A. Takahara, *Macromolecules*, 2005, **38**, 6316.
58. S. Ulrich and J.-M. Lehn, *Angew. Chem. Int. Ed.*, 2008, **47**, 2240.
59. M. Rikkou-Kalourkoti, K. Matyjaszewski and C. S. Patrickios, *Macromolecules*, 2012, **45**, 1313.
60. G. I. Litvinenko, P. F. W. Simon and A. H. E., Müller *Macromolecules*, 1999, **32**, 2410.
61. W. Tang, N. V. Tsarevsky and K. Matyjaszewski, *J. Am. Chem. Soc*., 2006, **128**, 1598.
62. K. Matyjaszewski, J. Pyun and S. G. Gaynor, *Macromol. Rapid Commun*., 1998, **19**, 665.
63. E. Daskalaki, B. L. Droumaguet, D. Gerard and K. Velonia, *Chem. Commun*., 2012, **48**, 1586.
64. B. S. Sumerlin and A. P. Vogt, *Macromolecules,* 2010, **43**, 1.
65. (a) M. A. Tasdelen, *Polym. Chem.,* 2011, **2**, 2133; (b) M. A. Tasdelen and Y. Yagci, *Angew. Chem. Int. Ed*., 2013, **52**, 5930.
66. (a) Y. Qi and A. Chilkoti, *Polym. Chem*., 2014, **5**, 266; (b) J. D. Wallat, K. A. Rose and J. K. Pokorski, *Polym. Chem*., 2014, **5**, 1545; (c) B. S. Sumerlin, *ACS Macro Lett*., 2012, **1**, 141.
67. H. Durmaz, M. Butun, G. Hizal and U. Tunca, *J. Polym. Sci., Part A: Polym. Chem*., 2012, **50**, 3116.
68. B. J. Adzima, C. J. Kloxin, C. A. DeForest, K. S. Anseth and C. N. Bowman, *Macromol. Rapid Commun*., 2012, **33**, 2092.